

# Carbon nanocage structures formed by one-dimensional self-organization of gold nanoparticles

Takeo Oku\* and Katsuaki Suganuma

Institute of Scientific and Industrial Research, Osaka University, Mihogaoka 8-1, Ibaraki, Osaka 567-0047, Japan.  
E-mail: Oku@sanken.osaka-u.ac.jp

Received (in Cambridge, UK) 15th July 1999, Accepted 25th October 1999

**Carbon nanocapsules and nanotubes have been formed by one-dimensional self-organization of gold nanoparticles, caused by the adhesive force at the step edge of amorphous carbon thin films; the present result is expected to be a promising fabrication technique for self-assembling nanowires and cluster-protected quantum dots at scales beyond the limits of current photolithography.**

The recent speed-up of ultra-large scale integrated circuits (ULSI) of semiconductor devices is highly dependent on the minimization of the design rule. New properties are also expected by formation of low dimensional arrays of quantum dots. The photolithography technique is used for the formation of these nanostructures, and ULSI with 0.07  $\mu\text{m}$  rule will be produced in 2009.<sup>1</sup> However, the limit of the design rule is reported to be 0.05  $\mu\text{m}$  (= 50 nm) using extreme ultraviolet lithography.<sup>2</sup> The establishment of nanostructure-formation technique by self-organization of nanoparticles<sup>3–8</sup> is worth investigation in order to overcome this lithography limit. However, self-organization has been of two- and three-dimensional type, whereas one-dimensional (1D) self-organization is required for the ‘nanowiring’ formation of the future ULSI devices.

The purpose of the present work is to form 1D carbon nanocage arrangements using self-organization of metal nanoparticles with a size below 10 nm. Gold colloids have been used for the formation of single electron transistors.<sup>9,10</sup> In the present work, gold (Au) nanoparticles were selected because of easy control of cluster size.<sup>11</sup> Fabrication of 1D Au nanodots and nanowires encapsulated in carbon nanocage structures was attempted by annealing the 1D self-organized nanoparticles on carbon thin films. In order to understand the self-organization mechanism, high-resolution electron microscopy (HREM)<sup>12,13</sup> was carried out. The present work gives a guideline for the design and synthesis of 1D self-organized nanostructures, which are expected for future nanoscale devices.

Au nanoparticles (ULVAC Ltd.) with a size of *ca.* 5 nm are selected in the present work for the 1D positioning. The surface of these nanoparticles was stabilized by  $\alpha$ -terpineol ( $\text{C}_{10}\text{H}_{18}\text{O}$ ) in toluene solution. The Au nanoparticle solution was dispersed on holey carbon grids with thickness *ca.* 15 nm (Oken Syoji. Co. Ltd.). After drying the specimens, they were loaded into the vacuum chamber and annealed at 400  $^{\circ}\text{C}$  for 30 min in a vacuum of *ca.*  $7 \times 10^{-4}$  Pa. HREM observations were performed with a 1250 kV electron microscope (ARM-1250) equipped with a top entry goniometer having a point-to-point resolution of 0.12 nm. To avoid sample damage by electron irradiation, the electron beam width for HREM observations was minimized by using a small spot size.

A low magnification image of as-prepared Au nanoparticles on amorphous carbon film is shown in Fig. 1(a). 1D ordering of Au nanoparticles with a size of 5 nm is observed over a length of 70 nm and a line profile of amorphous carbon across the row is shown. The image intensity of amorphous carbon at the lower side is 1.2 times stronger than that of the upper side as indicated by white lines in the inset to Fig. 1(a), which indicates that the step edge of the carbon thin films is *ca.* 3 nm ( $0.2 \times 15$  nm). The longest size of the 1D ordering was *ca.* 1.5  $\mu\text{m}$ , which is

dependent on the length of step edge of the carbon thin films. An enlarged HREM image of the self-organized Au nanoparticles is shown in Fig. 1(b). The image contrast of amorphous carbon in region A is brighter than that in region B, which also indicates the step edge of the carbon film as measured in Fig. 1(a). 1D positioning of Au nanoparticles with a width of *ca.* 15 nm is also observed in Fig. 1(c), which consists of two or three rows of Au nanoparticles. Reproducibility of the 1D self-organization was confirmed.

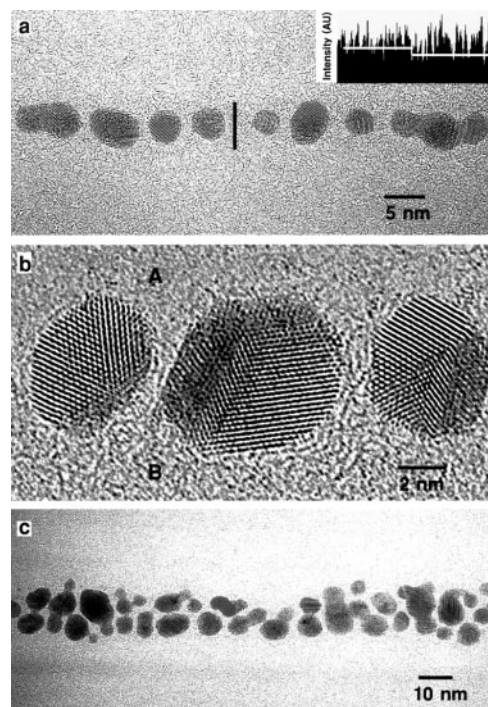


**Fig. 1** (a) Low magnification image of 1D self-organized Au nanoparticles on amorphous carbon film with the intensity distribution across the interface indicated. (b) Enlarged HREM image of 1D self-organized Au nanoparticles. (c) 1D self-organization of Au nanoparticles with a width of *ca.* 15 nm.

Fig. 2 shows HREM images of annealed Au nanoparticles at 400  $^{\circ}\text{C}$ . Au nanoparticles encapsulated in carbon nanocapsules are observed in Fig. 2(a). At elevated temperatures, Au nanoparticles grow by coalescence, and the particle size is *ca.* 15 nm. The carbon nanocapsules are isolated owing to the surface diffusion of Au and C atoms and the surface tension of the nanoparticles. Amorphous carbon would be graphitized by the catalytic effect<sup>14</sup> of the active Au surface at low temperature of 400  $^{\circ}\text{C}$  compared to that of ordinary chemical formation of carbon nanocapsules.<sup>15</sup> An enlarged image of the Au nanoparticles encapsulated in carbon nanocapsules is shown in Fig. 2(b). All the Au nanoparticles are surrounded and isolated by double or triple graphite sheets, which would prevent the nanoparticles from growing and so acts as cluster protection. Au nanowires encapsulated in carbon nanotubes are often formed as shown in Fig. 2(c). An Au nanoparticle encapsulated in a

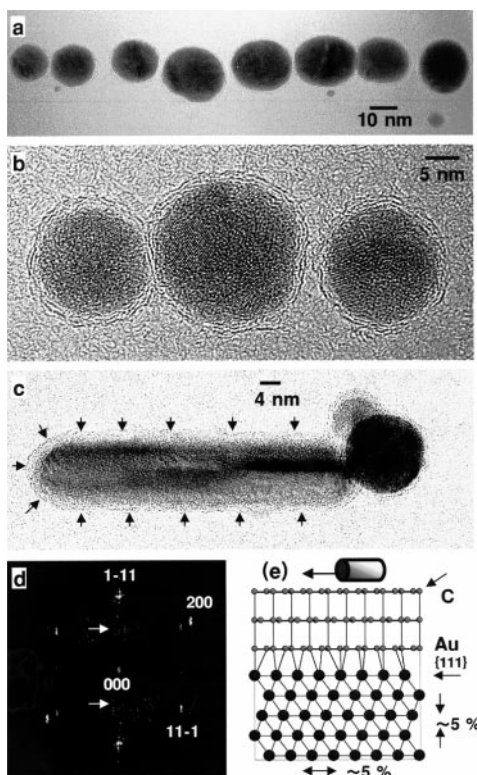


**Fig. 2** (a) Low magnification image of annealed Au nanoparticles at 400 °C. (b) HRTEM image of Au nanoparticles encapsulated in carbon nanocapsules. (c) Au nanowire encapsulated in carbon nanotube. (d) Fourier transformed pattern of the nanotube. (e) Structural model of Au{111}/C{002} interface.

carbon nanocapsule is also observed at the tip of the nanotube. The one-dimensionality is retained after the coalescence of nanoparticles, which is a useful formation technique for protected nanowires. The maximum length of the continuous wire is *ca.* 100 nm, and the length is dependent on the nanoparticle distance. A Fourier transformed pattern of a circular cross-section of a cut Au nanotube is shown in Fig. 2(d). The diffractogram is indexed with the [011] incidence of Au. In the Fourier transform, lattice distortion is observed as indicated by the streaks of each reflection perpendicular to the growth direction of the nanowire. Some distortion is observed in all Au nanowires. The 1 – 11 reflection is expanded, which indicates reduction of lattice distance of Au{111}. The maximum difference between 1 – 11 and 11 – 1 reflections is *ca.* 10%. Diffuse scattering of carbon 002 is observed as indicated by arrows, which is due to the carbon layers of the nanotube. A structure model of the Au{111}/C{002}<sub>nanotube</sub> interface is shown in Fig. 2(e). Lattice expansion and reduction are observed parallel and perpendicular to the growth axis, respectively. It is believed that the distortion of nanowire is due to the coalescence of nanoparticles along the growth direction at low temperatures. The maximum distortion is *ca.* 10%, which would indicate expansion and reduction of *ca.* 5%, respectively.

The formation of graphitic coatings around metal nanoparticles supported on amorphous-C films is often observed when subjected to high intensity electron beam irradiation.<sup>16</sup> However, a high intensity electron beam was not used here. As is evident in Fig. 1, which was obtained with a 1250 kV electron microscope, there are no graphite layers around the Au nanoparticles for the as-prepared samples. If the formation of the graphite layers around the nanoparticles is due to the effect of the electron beam, there should be carbon layers around the nanoparticles for the as-prepared samples. When a high intensity electron beam is used, an amorphous carbon matrix is also graphitized. However, an amorphous carbon matrix is observed around the carbon nanocapsules and nanotubes in Fig.

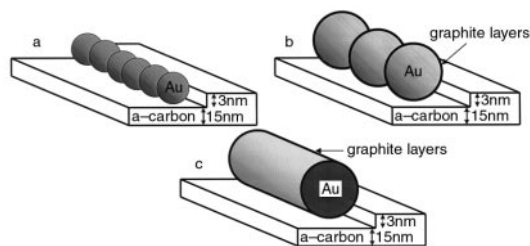


**Fig. 3** Schematic illustration of (a) 1D self-organized Au nanoparticles, (b) carbon nanocapsules and (c) a carbon nanotube.

2. In addition, several micrographs for the as-prepared and annealed samples were taken under the same conditions in the present work, and formation of carbon layers around the nanoparticles was observed only for the annealed samples. These results indicate that the formation of these carbon nanocage structures is due to annealing, and that this method is effective for the homogeneous formation of carbon nanocage structures.

A schematic illustration of self-organized Au nanoparticles, carbon nanocapsules and a carbon nanotube is shown in Fig. 3. Adhesion due to the step edge and substrate is the main force leading to the 1D arrangement whereas 2D self-organization<sup>6–8</sup> of nanoparticles is due to inter-nanoparticle forces by ligands around particles. The present result indicates that the 1D arrangement is strongly dependent on the step edge of the substrate. The formation of carbon nanocapsules and nanotubes would depend on the distance between gold nanoparticles. For larger distances, carbon nanocapsules will be formed while for smaller distances, gold nanowires will be formed by the coalescence of gold nanoparticles. Although step edges are formed by a simple sample preparation technique in the present work, the step edge size can be controlled by ordinary lithography techniques such as use of an electron beam, and is expected to be a viable nanofabrication technique for future electronic devices.

We acknowledge Professors K. Hiraga and E. Aoyagi for allowing us to use the electron microscope. This work was partly supported by The Shinsedai Foundation, and Grant-in-Aid for Scientific Research, Ministry of Education, Science, Sports and Culture, Japan.

## Notes and references

- 1 *National Technology Roadmap for Semiconductors*, The Semiconductor Industry Association, San Jose, CA, 1997.
- 2 J. E. Bjorkholm, J. Bokor, L. Eichner, R. R. Freeman, J. Gregus, T. E. Jewell, W. M. Mansfield, A. A. MacDowell, E. L. Raab, W. T. Silfvast, L. H. Szeto, D. M. Tennant, W. K. Waskiewicz, D. L. White, D. L. Windt and O. R. Wood II, *J. Vac. Sci. Technol. B*, 1990, **8**, 1509.
- 3 C. B. Murray, C. R. Kagan and M. G. Bawendi, *Science*, 1995, **270**, 1335.
- 4 C. A. Mirkin, R. L. Letsinger, R. C. Mucic and J. J. Storhoff, *Nature*, 1996, **382**, 607.
- 5 L. Motte, F. Billoudet, E. Lacaze, J. Douin and M. P. Pileni, *J. Phys. Chem. B*, 1997, **101**, 138.
- 6 Z. L. Wang, S. A. Harfenist, R. L. Whetten, J. Bentley and N. D. Evans, *J. Phys. Chem. B*, 1998, **102**, 3068.
- 7 C. J. Kiely, J. Fink, M. Brust, D. Bethell and D. J. Schiffrin, *Nature*, 1998, **396**, 444.
- 8 K. Pohl, M. C. Bartelt, J. de la Figuera, N. C. Bartelt, J. Hrbek and R. Q. Hwang, *Nature*, 1999, **397**, 238.
- 9 D. L. Klein, R. Roth, A. K. L. Lim, A. P. Alivisatos and P. L. McEuen, *Nature*, 1997, **389**, 699.
- 10 L. Feldheim and C. D. Keating, *Chem. Soc. Rev.*, 1998, **27**, 1.
- 11 G. Schmid, *Chem. Rev.*, 1992, **92**, 1709.
- 12 T. Oku and S. Nakajima, *Appl. Phys. Lett.*, 1999, **75**, 2226.
- 13 T. Oku and J.-O. Bovin, *Phil. Mag. A*, 1999, **79**, 821.
- 14 R. Lamber, N. Jaeger and G. Schulz-Ekloff, *Surf. Sci.*, 1988, **197**, 402.
- 15 T. Oku, K. Niihara and K. Sugauma, *J. Mater. Chem.*, 1998, **8**, 1323.
- 16 T. Oku, G. Schmid and K. Sugauma, *J. Mater. Chem.*, 1998, **8**, 2113.